Catalysis Communications 174 (2023) 106580

Contents lists available at ScienceDirect

Catalysis Communications

journal homepage: www.elsevier.com/locate/catcom

Pd as a reduction promoter for TiO_2: Oxygen and hydrogen transport at 2D and 3D Pd interfaces with TiO_2 monitored by TPR, *operando* ^1H NMR and CO oxidation studies

Melis Yarar, Asmae Bouziani, Deniz Uner *

Middle East Technical University, Chemical Engineering Department, 06800 Ankara, Turkiye

ARTICLE INFO

Keywords:
2D Pd/TiO_2
3D Pd/TiO_2
Hydrogen spillover
Oxygen reverse spillover
Operando NMR

ABSTRACT

Ambient temperature reduction of TiO_2 surface was observed through hydrogen spillover from Pd nanoparticles with a hydrogen consumption stoichiometry of 1.4 H_2:Pd up to ≤2 wt%Pd loading. This behavior was attributed to the formation of nanoparticles exhibiting 2D behavior for ≤2 wt%Pd loading. The 2D behavior of Pd nanoparticles were further confirmed from the relative abundance of metallic Pd in 3D, deduced from hydrogen stoichiometry of β-PdH_x. EPR revealed oxygen vacancy formation, *operando* NMR revealed facile hydrogen spillover, and CO oxidation reaction rates systematically increased for Pd ≤ 2 wt%, indicating facile exchange of hydrogen and oxygen at 2D Pd/TiO_2 interfaces.

1. Introduction

Titanium dioxide, owes its high reactivity due to the point defects like oxygen vacancies it can sustain. In 2011, Chen et al. [1] treated white titania powder under hydrogen atmosphere at high pressure and temperature, to observe a color change from white to black. The resultant material was accompanied with a highly defective structure and enhanced visible light absorption capability. This discovery was received enthusiastically by the catalysis community: the material could be activated under visible light, offering the potential of using solar energy for chemical conversions [2]. Visible light absorption and ability to catalyze new classes of reactions were attributed to a high content of oxygen vacancies and Ti^{+3} species [3]. Zhang et al. [2] showed that titania reduced at 600 °C under hydrogen flow for 3 h, exhibited visible light activity accompanied by enhanced durability. Similarly, Hu et al. [4] also reduced titania powders at 500 °C in hydrogen atmosphere for 3 h to demonstrate that particles have a narrower band gap and efficient visible light activity for several photocatalytic reactions.

It is widely known that deposition of a minute amount noble metals to the surface of reducible oxides alter the catalytic activity through a reduction promoter effect [5,6]. For example, Ru, used as a reduction promoter, ensures the reduced state of Co species on the surface. In the presence of Ru, reduction temperature of Co decreases as a result deactivation of Co surface during Fischer-Tropsch synthesis can be prevented [7]. In 2012 Jacobs et al. [8] reported that Pd is a better reduction promoter than Ru for Co based Fischer-Tropsch catalyst when cobalt oxide reduction temperature is considered, but with a drawback in terms of product selectivity. Similarly, Romero et al. [9] showed that, when applied in thin layers, Pd has the ability to promote reduction of Co even at room temperature. A similar study about Pd addition, in this case onto titania surface, was reported in 2016 by Xu et al. [10]: they reported that Pd could catalyze formation of defective and black-colored titania with mild temperature and low-pressure hydrogen treatment. Su et al. [11] studied titania reduced as such in order to analyze the effect of a disordered surface layer on visible light harvesting capacity. To the best of authors' knowledge, the principles behind Pd-catalyzed room temperature reduction of titania and effect of Pd loading and metal dispersion on the reducibility has yet to be demonstrated.

Dependence of catalytic activity on the particle size has been investigated by many since the very early times of supported catalyst research [12]. Surface thermodynamics dictate that adhesive forces are more dominant at low loadings. As the metal loading increases, cohesive forces between metal atoms start to dominate, leading to agglomeration of the particles and decreased interaction between metal and its support [13]. Haruta et al. [14] was one of the very first to establish the size effect by Au particles supported on titania for low temperature CO oxidation reaction. In particular, TOF was found to be increased as the diameter of Au particles increased up to 3 nm, then drastically decreased

* Corresponding author.
E-mail address: uner@metu.edu.tr (D. Uner).

https://doi.org/10.1016/j.catcom.2022.106580
Received 2 October 2022; Received in revised form 4 December 2022; Accepted 5 December 2022
Available online 8 December 2022

for $d_p > 3$ nm. Similar efforts were dedicated to explain effects of Pd loading, size and dispersion on catalytic activity of titania: Hutchings et al. [15] studied the subject for enantioselective hydrogenation of NADPME to obtain the best catalytic results at 2%Pd/TiO_2 at which the relationship between dispersion and particle size was optimized. Similarly, Al-Mazroai et al. [16] showed Pd loading on titania has a significant effect on rate of photocatalytic methanol reforming reaction which yielded the highest hydrogen production rate at 0.5% and no production from 4% and on which is explained by overlapping of metal particles at higher loadings that blocks the active site for the reaction.

In this study, we report experimental evidence through TPR, in situ ESR and *operando* ^{1}H NMR spectroscopy disclosing the role of Pd dispersion, especially the patches of atomically thin Pd formed at lower loadings towards the reduction of TiO_2 under low hydrogen pressures, ~0.13 bar, at room temperature. CO oxidation activity measurements at very low CO partial pressures revealed further evidence that the reaction takes place at the metal support interface.

2. Material and methods

2.1. Catalyst preparation

Pd was incorporated on TiO_2(P25-Degussa) by incipient wetness technique. 10% solution of palladium(*II*)nitrate($Pd(NO_3)_2$, 99.9%, Alfa Aesar) was diluted with sufficient amount of deionized water to bring about incipient wetness, the solution was mixed with TiO_2. The paste dried at room temperature overnight and at 120 °C for half an hour, before finely ground to a powder. Inductively coupled plasma-optical emission spectrometry (ICP-OES) was carried out to quantify the amount of Pd in the samples.

2.2. Temperature programmed analyses (TPx)

TPx experiments were performed on a Micromeritics Chemisorb 2720 equipment. The reactor filled with sample was placed in a furnace and the heating rate was fixed as 5 K/min, final temperature as 1000 K and gas flow rate as 25sccm (10% H_2 in Ar). Beneath the TPR reactor a Dewar filled with liquid nitrogen was placed to cool the sample to 220 K. The sample warmed up under natural forces, i.e., liquid nitrogen was allowed to boil off slowly, resulting in a slow but steady increase in temperature until room temperature is reached. Afterwards, heating by oven was started. Quantitative TPR Analyses were carried out for each sample using Ag_2O calibration, explained in Supporting Information (A2) in detail.

2.3. High resolution (HR) and high contrast (HC) transmission Electron microscopy

For each sample synthesized, High Resolution Transmission Electron Microscopy (HR-TEM) studies were conducted on Jem Jeol 2100F HRTEM (200 kV) while for High Contrast Transmission Electron Microscopy (HC-TEM) studies FEI Tecnai G2 Spirit BioTwin (20-120 kV) equipment was used.

2.4. Electron spin resonance spectroscopy (ESR) or Electron paramagnetic resonance (EPR) analysis

ESR Analysis was conducted with a Benchtop Bruker MicroESR. ESR tube was connected to a high vacuum (10^{-6} Torr) manifold made of Pyrex glass connected to a Varian Turbo V70D pump, described in detail elsewhere [17]. First, the ESR tube, filled with sample, was evacuated fully then H_2 gas at 100 Torr pressure was supplied at room temperature. Sample was treated with H_2 for half an hour four times and evacuation in-between each round, then the tube was evacuated overnight when the ESR spectrum was obtained with the following parameters at room temperature: 50 mW microwave power, 9.62 GHz frequency, 100 number of sweeps.

2.5. Nuclear magnetic resonance spectroscopy (NMR) analysis

A Magritek Spinsolve 43 MHz spectrometer was coupled to a vacuum manifold for *operando* ^{1}H NMR studies. Measurements were performed using Spinsolve Expert software for 1% and 5%Pd/TiO_2 samples. Prior to measurement, the sample was evacuated overnight and reduced with 300 Torr H_2 at room temperature for 3 h while time dependent NMR spectra were acquired while also recording the change in hydrogen gas pressure inside the sample tube.

2.6. CO oxidation measurements

Catalytic activity of Pd/TiO_2 samples at different Pd loadings were measured by CO oxidation reaction. A Pyrex reactor was loaded with 0.4 g of catalyst and connected to the gas manifold with MKS mass flow controllers on the upstream end and to a home built gas analyzer for quantitative CO and CO_2 detections on its downstream end. The CO sensor (maximum range 3% with 10 ppm resolution, Gascard NG/Edinburg Instruments), and CO_2 sensor (maximum range 10% with 0.01% resolution, Gascard NG/Edinburg Instruments) of the multi gas analyzer are NDIR type sensors equipped with a tungsten lamp as the infrared source. CO gas was supplied from a gas cylinder to the system with the flow rate fixed to 1.8 ml/min by a MKS mass flow controller calibrated with 200 sscm nitrogen gas and respective MFC readout. Air was supplied by a compressor and two gas streams were combined in a T-fitting by which they are sent to mixing chamber. At the outlet of mixing chamber another T-fitting divides the chamber outlet to two, one of which was exhaust to atmosphere and second is sent to a control valve. A control valve is used to adjust the reactor inlet flow rate to 180 ml/min air and CO mixture with a CO concentration around 1100 ppm. The reactor was heated using a hot plate between room temperature to 300 °C for thermal activity measurements. This system was designed for simultaneous activation by thermal and photo activity measurements; hence a hot plate was installed which allows simultaneous UV or visible light irradiation and heat input (Fig.S1).

3. Results and discussion

3.1. TPR and HR and HC-TEM analyses

H_2-TPR profiles of pure and 0.5, 1, 2, 5 and 10%Pd containing TiO_2 samples are given in Fig. 1; the features after 350 K were magnified by a factor 10 for Pd/TiO_2 and 100 for TiO_2 for better visualization. Pure titania sample was found to be reduced showing two peaks: one very vague at 400 K and a broader one centered at 800 K of which was assigned as surface reduction, consistent with previously reported TPR results in literature [18]. On the other hand, TPR profile of 1%Pd/TiO_2 shows four positive peaks at 280 K, 300 K, 600 K, 800 K in addition to the negative peak at 340 K which was assigned to PdH decomposition.

In the beginning of the TPR, Pd is present as PdO requiring the same number of moles of H_2 to completely reduce PdO species through the reaction PdO → Pd + H_2O. The quantitative analysis of each peak was carried out against silver oxide calibration (SI.A2). The quantitative comparison of the first sharp peak around 280 K was quantified to obtain a H_2/Pd ratio of 1.09. The excess amount of hydrogen was interpreted as hydrogen consumed to form PdH. When the hydride decomposition peak was quantified, the material balance of hydrogen was closed, confirming quantitative consistency of our methodology.

Since the amount of H_2 consumed for the first peak is equal to the amount H_2 needed for PdO reduction and formation of PdH phase, it is concluded that full reduction of PdO and production of hydride phase is completed around 280 K. The remaining peaks then should be attributed to the reduction events on TiO_2. In addition to appearance of these new peaks, decrease in reduction temperature as well as a significant

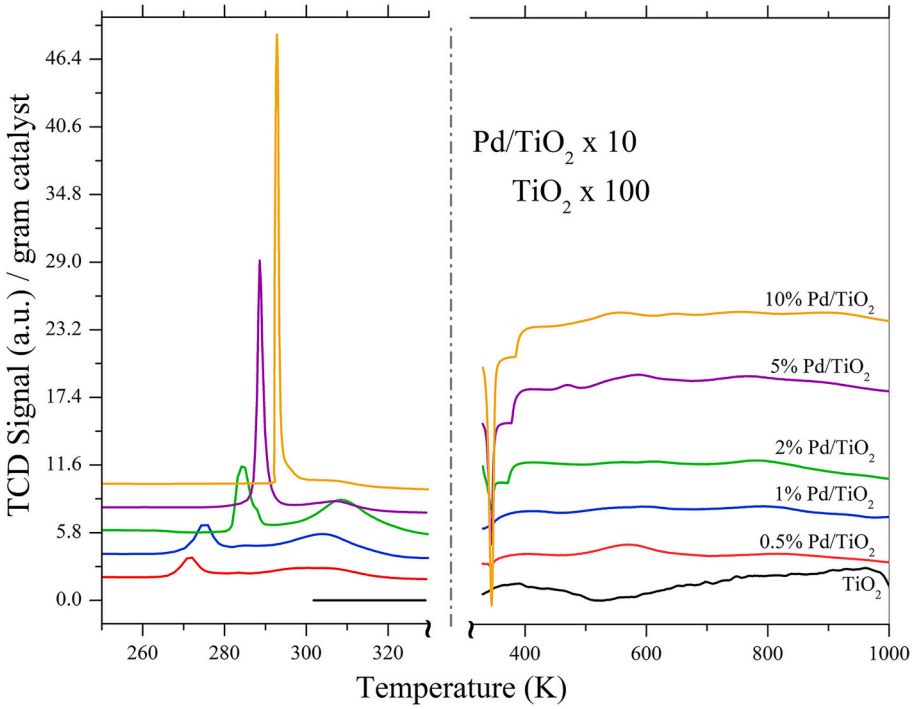

Fig. 1. H_2-TPR profile of pure and Pd/TiO_2. The features after 350 K were magnified by a factor of 10 or 100 for better visualization.

increase in reduction of titania after Pd incorporation was observed. In fact, when quantitative analysis of TPR peaks in the range 400 K < T < 1000 K were carried out (Table S1), it was found that the amount of pure titania reduced was 0.93%, this value increased to 4.57% after 1%Pd was added. Following the early reports of Khoobiar [19] and Boudart et al. [20] on migration of dissociated hydrogen atoms by noble metals onto the neighboring material, this reduction was interpreted to be due to spillover.

The new TPR peaks identified for 1% Pd containing sample were also identified for the other Pd containing samples as seen in Fig. 1. It was further established that TPR peaks corresponding to PdO reduction and decomposition of β-PdH assignments were also consistent with the literature [21]. The effect of Pd loading on hydrogen consumption for the peaks attributed to PdO reduction and PdH decomposition are available in SI (Fig.S4.a and Fig.S4.b respectively).

The stoichiometries for the formed hydride phases were found as $PdH_{0.09}$, $PdH_{0.19}$, $PdH_{0.37}$, $PdH_{0.41}$ $PdH_{0.53}$ by quantitative analysis, for 0.5, 1, 2, 5 and 10%Pd/TiO_2, respectively. Bulk β-PdH is expected to have 0.53 > (H/Pd) stoichiometry [22]. This stoichiometry could not be reached at low Pd loadings. This was interpreted to be due to the absence of a full 3D bulk Pd structures. An estimation based on expected PdH stoichiometry (0.53) and that measured by TPR hydride peaks were reported in Table 1. The missing amounts of hydrogen was interpreted as Pd that is not available in 3D. In other words, H:Pd stoichiometries refer to Pd that exist in bulk phase Pd while the rest of Pd that would add up to H/Pd = 0.53 is in 2D form(Table 1).

On the H_2-TPR profiles of Pd containing samples, a distinct reduction peak was observed for 0.5 < %wt.Pd < 5 loadings around 300 K and quantitative analysis reveal the behavior of hydrogen consumption in this peak with respect to Pd amount (Fig. 2). The reduction of Pd, formation of βPdH and its decomposition were complete before this peak appeared. Hence, this peak is attributed to a low temperature reduction of TiO_2 through dissociated H_2 spilled over from Pd acting as a reduction promoter. The Pd amounts that is estimated to be 2D were presented in the last column of Table 1. This data strongly correlates with the experimental hydrogen consumption data presented in Fig. 2, with the exception of 5 wt% loaded catalyst.

Table 1
Pd intended coverages and estimation of Pd Amounts in bulk 3D from βPdH Stoichiometry.

Pd loading (%)	Intended % Pd coverage (ML)[a]	H/Pd estimated from βPdH peak	Bulk metallic Pd amount that can give rise to βPdH (%)[b]	Rest of Pd that is not 3D (%)	mmol Pd atoms/g catalyst that is not 3D[c]
0.5	0.06	0.09	17	83	3.9
1	0.11	0.19	36	64	6.0
2	0.23	0.37	69	31	5.8
5	0.57	0.41	77	23	10.8
10	1.14	0.53	99	1	0.9

[a] Estimation is crudely based on 10^{15} atom/cm^2 approximation, 50 m^2/g TiO_2 surface area.
[b] Estimation is based on finding the amount of Pd that can have 0.53H:Pd stoichiometry.
[c] Estimation is based on the metal loading and %Pd that is not in 3D.

BET surface area of TiO_2 is 50 m^2/g corresponding to an estimated 6.63% of sites at the surface. A quantitative analysis for 1%Pd/TiO_2 revealed that the peaks at 300 K and 595 K consumed sufficient amount of hydrogen to reduce 6.67% of TiO_2 (Table S1). Therefore, the peaks at 300 K and 595 K were assigned to to surface reduction. The peak at 300 K constitutes roughly 70% of the total hydrogen consumption, rest is consumed at 595 K.

The data in Fig. 2 exhibit a maximum at 2%Pd. The maximum is attributed to the availability of the interface between Pd and TiO_2, especially through 2D particles. HRTEM images reveal that at loadings up to 2%, Pd is well dispersed and patches with 2D structure can be identified. Therefore, we conclude that up to 2%Pd, increased loading increases the interface area between Pd and TiO_2. As a result, the rate of atomic transfer via hydrogen spillover between metal and support and reducibility of TiO_2 is enhanced. At higher loadings, Pd particles begin to agglomerate, the Pd morphology changes from 2D to 3D dominant character, lowering the Pd/TiO_2 interface hence the reducibility of TiO_2. Once metal particles decorated on oxide surfaces are thin enough and if the particles located on close enough perimeter of oxide species, the

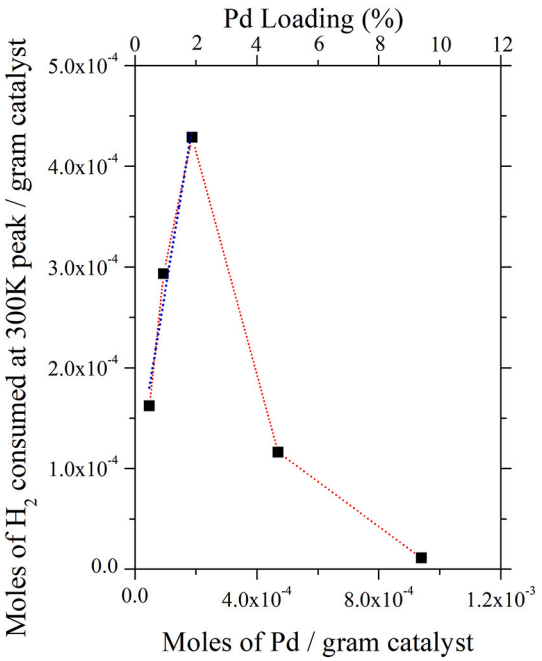

Fig. 2. Moles of H_2 consumed at 300 K peak per gram catalyst vs moles of Pd per gram catalyst curve exhibit a maximum for 2% Pd/TiO_2 loadings.

adsorbed gas can diffuse from metal sites to oxide surfaces more expeditiously than their bulk counterparts [28]. In that case, in monolayer metals on oxide surfaces, metal particles maintain a strong metallic bond in only two dimensions while they do not possess any in the third dimension which split their valence bands in two different orientations that result in highly stable and active metals in catalysis applications [24]. Hence, we report here that in the case of 0.5, 1 and 2%Pd/TiO_2 thinner Pd layer justify the smoothness of the atomic diffusion process between Pd and titania species.

For 0.5, 1 and 2%Pd/TiO_2 moles of H_2 consumed at 300 K TPR peak shows a linear correlation to the amount of Pd with a slope of 1.4(=H_2: Pd), fitted line is indicated as a blue dashed line in Fig. 2. One H_2 molecule can capture one oxygen atom from surface: Hence it can be concluded that 2D Pd particles have the ability to reduce the same amount of titania surface species as Pd atoms present on the surface at room temperature while this is not the case for 3D Pd particles.

The TEM data (given in SI, Fig. S5 and S6) indicates the presence of Pd and titania particles characterized by lattice fringes of 0.24 nm and 0.33 nm [18]. Pd particle sizes was observed to be reaching up to 12 nm for 0.5 wt% Pd loadings (Fig. S6 a and b) which indicate formation of patches of atomically thin metal structures on the titania surface [23,24]. In addition, 3D Pd particles could be observed for 1% sample (Fig.S5.b) which proves the co-existence of 2D and 3D metal structures on low Pd loaded samples, in line with the TPR analysis of PdH decomposition peak. TEM images also revealed large agglomerated, Pd nano-particles at loadings higher than 2% (Fig.S5.c). Analogues to the results deduced here which proves Pd particles change phases from 2D to 3D as the amount of metal incorporated on support is increased, loading is shown to be altering the 2D—3D structure of metals by Liu et al. [25] and references there in. In particular, Roca and Kamiya [26] also observed by AFM studies that 2D InAs particles agglomerate as 3D when the amount is increased.

An early STM study of nucleation and growth of Pd over TiO_2 (110) [27] revealed Volmer Weber mode of Pd growth on TiO_2 single crystals. In other words, the crystal growth mode transitions from 2D to 3D at a Pd coverage of 0.012 ML, 80% of the crystals are of atomic layer thick with the presence of 3D geometries. In the same study, experimental bandgap data indicated that the onset of metallic behavior started when the clusters are larger than 385 atoms, consistent with the estimations in this study.

3.2. ESR analysis

In order to affirm room temperature reducibility of Pd supported titania, in situ ESR experiments at ambient temperature were performed (Fig. 3). On the contrary to pure TiO_2 and 10%Pd/TiO_2; 0.5%Pd/TiO_2 which exposed to low-pressure (~0.13 bar) and room temperature hydrogen treatment and evacuated afterwards, possess paramagnetic centers. The signal around 3500G($g < 1.98$) was attributed to Ti^{+3} species and other sharp signal around 3450G($g = 2.00$) which corresponds to a signal emanating from a free electron due to oxygen vacancies [29]. Oxygen vacancy signal revealed an intimate interaction of 0.5% Pd with TiO_2. These results further indicate that, at low Pd loadings, atomically thin layers of Pd particles can form, these particles assist the reduction of titania surface even under mild temperatures and low hydrogen pressures. It was not possible to observe oxygen vacancies obtained with this treatment unless the system was fully evacuated, since only in vacuum the thermal motion of particles was slow enough to provide a significant signal narrowing that allow detection of paramagnetic centers which is not possible at high pressures [30]. Furthermore, when the sample that exhibited the ESR signal due to the oxygen vacancy was exposed to ambient conditions the signal was no longer observable. This is attributed to fast annihilation of oxygen vacancies through the Pd sites.

3.3. Operando NMR studies

Operando ^{1}H *NMR* Spectroscopy of 1%Pd/TiO_2 at room temperature and hydrogen pressure was recorded as a function of time and hydride phase of palladium and hydroxyl species formed upon hydrogen interaction are seen with peaks at 27.4 and 4.74 ppm, respectively (Fig. 4). The procedure was repeated for 5%Pd/TiO_2 in a similar manner (Fig. S7). For both of the samples, hydroxyl signal was found to be growing with time. The sole source of hydrogen atoms in the hydroxyl species is the hydrogen gas present in the system. Hence, cumulatively adsorbed amount of hydrogen was calculated from chemisorption measurements and compared to NMR signal area of hydroxyl peak. The parity plot is strictly linear indicating strong correlation between hydrogen consumption form the gas phase and increase in hydroxyl signals on the

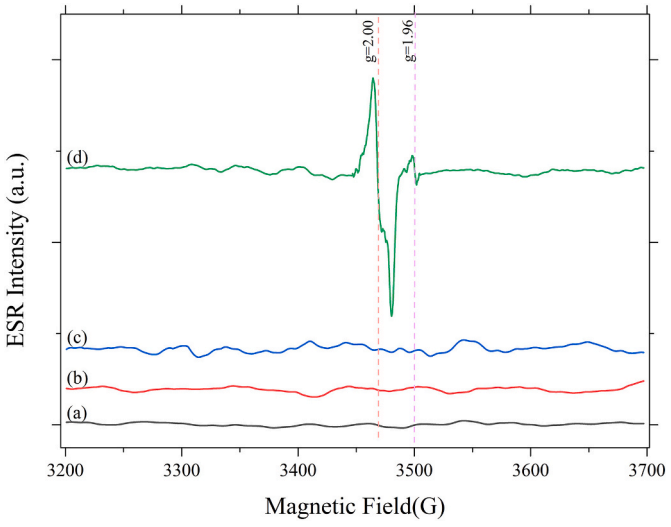

Fig. 3. ESR spectra of (a) TiO_2 in air, (b) 0.5% Pd/TiO_2 in H_2 atmosphere, (c) 10% Pd/TiO_2 in vacuum after mild H_2 treatment, (d) 0.5% Pd/TiO_2 in vacuum after mild H_2 treatment reveal the role of Pd at low loadings in creating oxygen vacancies.

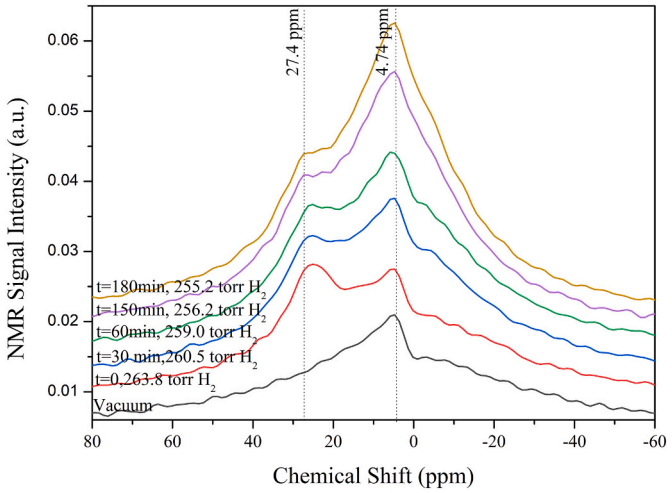

Fig. 4. Time dependent ^{1}H NMR spectra of 1%Pd/TiO_2under 260 Torr initial hydrogen pressure. Pressure decrease indicates adsorption and hydrogen migration processes are facile.

surface (Fig.S8).

Considering hydrogen spillover, the process is diffusion dependent since, hydrogen migrates through Pd layer to reach metal-support interface. Therefore, the amount of hydrogen atoms contributing to the formation of hydroxyl species has to be equal to the number hydrogen migrated through Pd layer to the interface. From this point of view NMR signal area is used as a measure of relative rate of atomic transport between Pd and titania surface for 1% and 5%Pd/TiO_2. The normalized area of hydroxyl signal (against hydroxyl signal area of untreated samples in vacuum) per Pd gram present in catalysts for these two samples were compared in Fig. 5. A sharper increase at the beginning of hydrogen exposure is seen for 1% sample. This suggests that interface between Pd and titania has a higher surface area on 1%Pd/TiO_2 sample than 5% and consequently on 1%Pd/TiO_2 the faster hydrogen migration between the two is possible which leads to an accelerated rate of hydroxyl formation. On the other hand, after 1800 s, the slopes of hydroxyl formation rate of two samples are equalized. After that point process is no longer dependent on Pd particles on support, consequently hydrogen started to be accumulated and migrated on titania surface. Our results are supported by evidence from the literature indicating the rate of spillover process increase with increasing interface between metal-support [31]. Additionally, small metal particles were shown to be the dominant source of spillover while agglomerated particles found not to take a part in the process [32].

3.4. CO oxidation measurements

CO oxidation reaction was run under 180 ml/min 1100 ppm CO in air mixture at room temperature, 100, 200 and 300 °C. An example of how CO and CO_2 concentration changes at the outlet of the reactor is given in Fig.S9 for a sample run and results of CO conversion analyses are given in Fig. 6. The data indicate that as the Pd loading is increased from 0.5% to 2%, the activity increases. Further increase in loading to 10% does not influence the catalytic activity any further. This behavior is attributed to the role of oxygen between TiO_2 and Pd interface, that is accessible to CO oxidation reaction.

According to Meng et al. [33], CO oxidation over Pd supported on oxide proceeds through reaction between CO adsorbed on Pd and an oxygen atom on support surface to produce CO_2. Following this hypothesis, Pd-TiO_2 interface area must be as high as possible to give rise to increased CO oxidation rate. Changes in CO conversion from 0.5% to 2% is higher than change in conversion from 2% to 10%. In other words, increase in Pd amount is reflected on increase in CO conversion values between 0.5% to 2% which are samples with 2D Pd features and high dispersion, while it was not the case for 2% to 10% which is the sample with 3D nanostructure. Consequently, it is reasonable to conclude that increase in Pd amount increases CO oxidation rate in 2D phase region due to enhanced interaction between metal and support however, when the Pd structure is changed to 3D no significant rate enhancement is possible with increasing Pd amount. Previously, Kolobov et al. [34] showed when Pd/titania system in the region of 0.05%–2% metal loading was investigated, oxidation activity was found to be increasing with increasing Pd loading. Similarly, Selishchev et al. [35] reports the same trend for Pd loadings between 0 and 4%.

It must be noted here that, CO oxidation experiments were repeated under visible light excitation coupled to a thermal excitation. No activity in the visible light region could be measured. Hence, we conclude that the oxygen vacancies created by a reduction promoter may not be as stable as their counterparts synthesized under high temperature and pressure conditions, also supported by our ESR data.

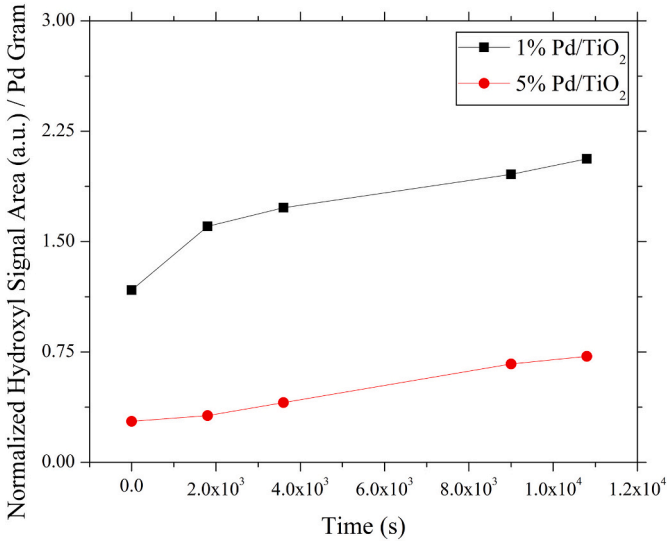

Fig. 5. NMR quantitative analysis for 1%Pd/TiO_2 and 5%Pd/TiO_2 revealing the role of the metal support interface for the spillover process.

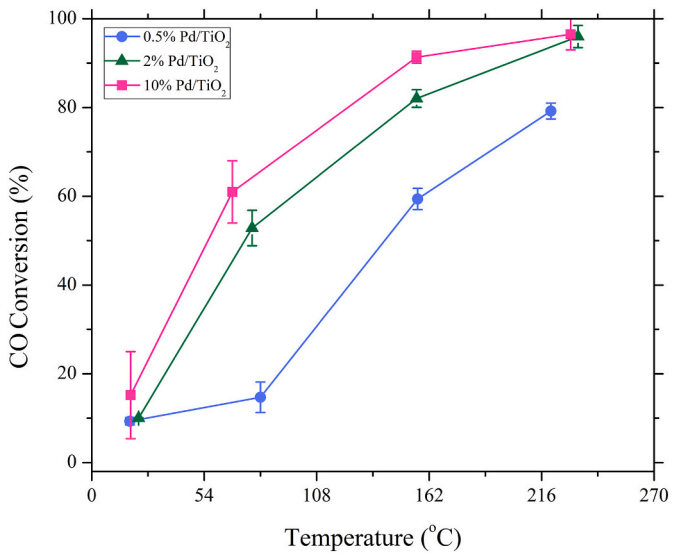

Fig. 6. Results of CO oxidation catalytic tests for CO conversion.

4. Conclusions

Interaction of hydrogen with titania in the presence of Pd gave rise to a TPR peak attributed to surface reduction of TiO_2 at 300 K. At low Pd loadings (≤2 wt%) hydrogen consumption stoichiometry of this peak scaled linearly with Pd amount with a stoichiometry of 1.4 H_2:Pd. At higher Pd loadings increasing Pd amounts decreased the H_2:Pd stoichiometry of this peak. This reduction behavior was combined with the evidence from TEM data, and interpreted as formation of patches of atomically thin layers of Pd at low Pd loadings. The peak observed at 300 K was attributed to the reduction of titania with spilled over hydrogen, primarily originated from 2D patches of Pd. The close interaction for samples with 2D features could account for enhanced H transport to support, leading to reduction of titania surface at room temperature and low-pressure. This interpretation was corroborated through the β-PdH stoichiometry: at low Pd loadings the stoichiometry was lower than 0.53H:Pd, indicating the scarcity of bulk Pd with a metallic behavior at lower loadings. Furthermore, the light-off activity of these catalysts for CO oxidation reaction indicated an increase in activity with increasing Pd amount up to 2 wt%. Further increase in metal loading did not cause an appreciable increase in activity. This result also corroborated our interpretation that further increase than 2 wt% in Pd loading triggered the formation of 3D structures with no improvement in the CO oxidation activity of the catalyst taking place at the metal support interface.

CRediT authorship contribution statement

Melis Yarar: Conceptualization, Methodology, Software, Validation, Formal analysis, Investigation, Data curation, Writing – original draft, Writing – review & editing. **Asmae Bouziani:** Investigation, Validation, Writing – original draft. **Deniz Uner:** Conceptualization, Methodology, Formal analysis, Resources, Data curation, Writing – review & editing, Supervision, Project administration, Funding acquisition.

Declaration of Competing Interest

The authors declare that they have no known competing financial interests or personal relationships that could have appeared to influence the work reported in this paper.

Data availability

Data will be made available on request.

Acknowledgment

Funding for this work is provided by TUBITAK grants 117M040 of 1001 program and 120C150 National Leader Researcher Program.

Appendix A. Supplementary data

Supplementary data to this article can be found online at https://doi.org/10.1016/j.catcom.2022.106580.

References

[1] X. Chen, L. Liu, P.Y. Yu, S.S. Mao, Increasing solar absorption for Photocatalysis with black hydrogenated titanium dioxide nanocrystals, Science 331 (2011) (1979) 746–750, https://doi.org/10.1126/science.1200448.
[2] K. Zhang, W. Zhou, X. Zhang, B. Sun, L. Wang, K. Pan, B. Jiang, G. Tian, H. Fu, Self-floating amphiphilic black TiO2 foams with 3D macro-mesoporous architectures as efficient solar-driven photocatalysts, Appl Catal B. 206 (2017) 336–343, https://doi.org/10.1016/J.APCATB.2017.01.059.
[3] G. Wang, H. Wang, Y. Ling, Y. Tang, X. Yang, R.C. Fitzmorris, C. Wang, J.Z. Zhang, Y. Li, Hydrogen-treated TiO2 nanowire arrays for photoelectrochemical water splitting, Nano Lett. 11 (2011) 3026–3033, https://doi.org/10.1021/nl201766h.
[4] M. Hu, Z. Xing, Y. Cao, Z. Li, X. Yan, Z. Xiu, T. Zhao, S. Yang, W. Zhou, Ti3+ self-doped mesoporous black TiO2/SiO2/g-C3N4 sheets heterojunctions as remarkable visible-lightdriven photocatalysts, Appl Catal B. 226 (2018) 499–508, https://doi.org/10.1016/J.APCATB.2017.12.069.
[5] S.L. Soled, E. Iglesia, R.A. Fiato, J.E. Baumgartner, H. Vroman, S. Miseo, Control of metal dispersion and structure by changes in the solid-state chemistry of supported cobalt Fischer–Tropsch catalysts, Top. Catal. 26 (2003) 101–109, https://doi.org/10.1023/B:TOCA.0000012990.83630.f9.
[6] D.O. Uner, M. Pruski, T.S. King, The role of alkali promoters in Fischer-Tropsch synthesis on Ru/SiO2 surfaces, Top. Catal. 2 (1995) 59–69, https://doi.org/10.1007/BF01491955.
[7] E. Iglesia, S.L. Soled, R.A. Fiato, G.H. Via, Bimetallic synergy in cobalt ruthenium Fischer-Tropsch synthesis catalysts, J. Catal. 143 (1993) 345–368, https://doi.org/10.1006/jcat.1993.1281.
[8] G. Jacobs, W. Ma, P. Gao, B. Todic, T. Bhatelia, D.B. Bukur, S. Khalid, B.H. Davis, Fischer-tropsch synthesis: differences observed in local atomic structure and selectivity with pd compared to typical promoters (Pt, re, Ru) of co/Al 2O 3 catalysts, Top. Catal. 55 (2012) 811–817, https://doi.org/10.1007/s11244-012-9856-5.
[9] C.P. Romero, J.I. Avila, R.A. Trabol, H. Wang, A. Vantomme, M.J. van Bael, P. Lievens, A.L. Cabrera, Pd as a promoter to reduce co cluster films at room temperature, Int. J. Hydrog. Energy 35 (2010) 2262–2267, https://doi.org/10.1016/j.ijhydene.2010.01.026.
[10] Y. Xu, C. Zhang, L. Zhang, X. Zhang, H. Yao, et al., Pd-catalyzed instant hydrogenation of TiO2 with enhanced photocatalytic performance, energy, Environ. Sci. 9 (2016) 2410–2417, https://doi.org/10.1039/c6ee00830e.
[11] Y. Su, J. Cao, L. Li, G. Zhang, P. Zheng, TiO 2 hollow spheres with surface-rich Ti 3 + under Pd-catalyzed hydrogenation for improved visible-light photocatalysis, J. Nanopart. Res. 21 (2019), https://doi.org/10.1007/s11051-019-4470-0.
[12] M. Che, C.O. Bennett, The Influence of Particle Size on the Catalytic Properties of Supported Metals, 1989, pp. 55–172, https://doi.org/10.1016/S0360-0564(08)60017-6.
[13] G.C. Bond, The origins of particle size effects in heterogeneous catalysis, Surf. Sci. 156 (1985), https://doi.org/10.1016/0039-6028(85)90273-0.
[14] M. Haruta, S. Tsubota, T. Kobayashi, H. Kageyama, M.J. Genet, B. Delmon, Low-temperature oxidation of CO over gold supported on TiO2, α-Fe2O3, and Co3O4, J. Catal. 144 (1993), https://doi.org/10.1006/jcat.1993.1322.
[15] N.J. Coulston, R.P.K. Wells, P.B. Wells, G.J. Hutchings, Enantioselective hydrogenation of N-acetyl dehydrophenylalanine methyl ester using cinchonine-modified Pd/TiO2 catalysts, Catal. Today 114 (2006) 353–356, https://doi.org/10.1016/J.CATTOD.2006.02.039.
[16] L.S. Al-Mazroai, M. Bowker, P. Davies, A. Dickinson, J. Greaves, D. James, L. Millard, The photocatalytic reforming of methanol, Catal. Today 122 (2007) 46–50, https://doi.org/10.1016/J.CATTOD.2007.01.022.
[17] D. Uner, N.A. Tapan, I. Özen, M. Üner, Oxygen adsorption on Pt/TiO2 catalysts, Appl. Catal. A Gen. 251 (2003) 225–234, https://doi.org/10.1016/S0926-860X(03)00317-X.
[18] W. Liang, X. Du, Y. Zhu, S. Ren, J. Li, Catalytic oxidation of chlorobenzene over Pd-TiO2 /Pd-Ce/TiO2 catalysts, Catalysts. 10 (2020), https://doi.org/10.3390/catal10030347.
[19] S. Khoobiar, Particle to particle migration of hydrogen atoms on platinum—alumina catalysts from particle to neighboring particles, J. Phys. Chem. 68 (1964), https://doi.org/10.1021/j100784a503.
[20] A.J. Robell, E.V. Ballou, M. Boudart, Surface diffusion of hydrogen on carbon, J. Phys. Chem. 68 (1964) 2748–2753, https://doi.org/10.1021/j100792a003.
[21] U.S. Ozkan, M.W. Kumthekar, G. Karakas, Characterization and temperature-programmed studies over Pd/TiO2 catalysts for NO reduction with methane, Catal. Today 40 (1998) 3–14, https://doi.org/10.1016/S0920-5861(97)00112-0.
[22] F.D. Manchester, A. San-Martin, J.M. Pitre, The H-Pd (hydrogen-palladium) system, J. Phase Equilib. 15 (1994) 62–83, https://doi.org/10.1007/BF02667685.
[23] Z. Cui, X. Bai, Ultrasonic-assisted synthesis of two dimensional coral-like Pd nanosheets supported on reduced graphene oxide for enhanced electrocatalytic performance, Ultrason. Sonochem. 70 (2021), 105309, https://doi.org/10.1016/J.ULTSONCH.2020.105309.
[24] J. Jiang, W. Ding, W. Li, Z. Wei, Freestanding single-atom-layer Pd-based catalysts: oriented splitting of energy bands for unique stability and activity, Chem. 6 (2020) 431–447, https://doi.org/10.1016/j.chempr.2019.11.003.
[25] P. Liu, Y. Zhao, R. Qin, S. Mo, G. Chen, L. Gu, D.M. Chevrier, P. Zhang, Q. Guo, D. Zang, B. Wu, G. Fu, N. Zheng, Photochemical route for synthesizing atomically dispersed palladium catalysts, Science 352 (2016) (1979) 797–800, https://doi.org/10.1126/science.aaf5251.
[26] R.C. Roca, I. Kamiya, Change in topography of InAs submonolayer nanostructures at the 2D to 3D transition, Phys. Status Solidi B 258 (2021) 2000349, https://doi.org/10.1002/pssb.202000349.
[27] C. Xu, X. Lai, G.W. Zajac, D.W. Goodman, Scanning tunneling microscopy studies of the TiO2(110) surface: structure and the nucleation growth of Pd, Phys. Rev. B 56 (1997) 13464–13482, https://doi.org/10.1103/PhysRevB.56.13464.
[28] C.T. Campbell, Ultrathin metal films and particles on oxide surfaces: structural, electronic and chemisorptive properties, Surf. Sci. Rep. 27 (1997) 1–111, https://doi.org/10.1016/S0167-5729(96)00011-8.
[29] J.B. Priebe, J. Radnik, A.J.J. Lennox, M.M. Pohl, M. Karnahl, D. Hollmann, K. Grabow, U. Bentrup, H. Junge, M. Beller, A. Brückner, Solar hydrogen production by plasmonic au-TiO2 catalysts: impact of synthesis protocol and TiO2 phase on charge transfer efficiency and H2 evolution rates, ACS Catal. 5 (2015) 2137–2148, https://doi.org/10.1021/cs5018375.

[30] M. Yarar, D. Üner, Oxygen vacancies on Pd/TiO2 are detected at low pressures by ESR spectroscopy at ambient temperatures, Turk. J. Chem. 46 (2022) 1081–1088, https://doi.org/10.55730/1300-0527.3416.
[31] Y.Y. Wu, N.A. Mashayekhi, H.H. Kung, Au-metal oxide support interface as catalytic active sites, Catal, Sci. Technol. 3 (2013) 2881–2891, https://doi.org/10.1039/c3cy00243h.
[32] J.M. Cíes, J.J. Delgado, M. López-Haro, R. Pilasombat, J.A. Pérez-Omil, S. Trasobares, S. Bernal, J.J. Calvino, Contributions of electron microscopy to understanding CO adsorption on powder au/ceria-zirconia catalysts, Chem. Eur. J. 16 (2010) 9536–9543, https://doi.org/10.1002/chem.201000866.
[33] L. Meng, A.-P. Jia, J.-Q. Lu, L.-F. Luo, W.-X. Huang, M.-F. Luo, Synergetic effects of PdO species on CO oxidation over PdO–CeO2 catalysts, J. Phys. Chem. C 115 (2011) 19789–19796, https://doi.org/10.1021/jp2056688.
[34] N.S. Kolobov, D.S. Selishchev, A.V. Bukhtiyarov, A.I. Gubanov, D.V. Kozlov, UV-LED photocatalytic oxidation of CO over the Pd/TiO2 catalysts synthesized by the decomposition of Pd(acac)2, Mater Today Proc. 4 (2017) 11356–11359, https://doi.org/10.1016/j.matpr.2017.09.008.
[35] D.S. Selishchev, N.S. Kolobov, A.V. Bukhtiyarov, E.Y. Gerasimov, A.I. Gubanov, D. V. Kozlov, Deposition of Pd nanoparticles on TiO2 using a Pd(acac)2 precursor for photocatalytic oxidation of CO under UV-LED irradiation, Appl Catal B. 235 (2018) 214–224, https://doi.org/10.1016/j.apcatb.2018.04.074.